https://doi.org/10.48048/tis.2024.7402

Study and Characterization of Copper and Titanium Oxides Nanostructures for Some Molecular and Biological Applications

Omar Abdulazeez Alhamd[1], Ghazwan Ghazi Ali [2*] and Mutaz Salih Hasan Aljuboori[2]

[1]Department of Biology, College of Education for Pure Sciences, University of Mosul, Mosul, Iraq
[2]Department of Physics, College of Education for Pure Science, University of Mosul, Mosul, Iraq

([*]Corresponding author's e-mail: dr.ghazwan39@uomosul.edu.iq)

Received: 18 August 2023, Revised: 5 September 2023, Accepted: 20 September 2023, Published: 5 February 2024

Abstract

In this work, Copper and Titanium nanocomposites (NPs) were prepared by mixture exchange process with ratios (25, 50 and 75 % CuO-TiO_2). The biological activity was studied, and it was found that the concentrations of 50 and 100 µg/mL of 50 and 75 % CuO-TiO_2 were the best concentrations, Low concentrations of the nanoparticle mixture at 25 µg/mL also stimulated the growth of symbiotic bacteria. The mixture of nanoparticles was easier to prepare and more effective in inhibiting bacterial growth. biochemical test and PCR were performed to confirm the identity of the studied bacteria. While isolating the bacteria, a new type of bacteria was detected and registered in the Global Gen Bank under accession No. OP942239. Surface and structure properties have been studied using FESEM, EDS analysis, XRD and FTIR respectively. It can be seen that the size and diameter of the nanocomposite increase with the weight ratio of CuO-TiO_2. The aggregated CuO-TiO_2 nanostructures with different ratios were transformed gradually into a uniform spherical shape. The average size of the CuO/TiO_2 composite was found to be about 32.122, 29.865 and 27.607 nm at 25, 50 and 75 % CuO-TiO_2 respectively. While the mean sizes of CuO and TiO_2 were 25.35 and 34.38 nm respectively. The crystalline size decreases after the ion exchange process, which could be due to the diffraction peaks being broad in all the samples of Copper Titanate at the surface. Subsequently, adding Copper particles to the TiO_2 film can improve the performance of the material.

Keywords: Antibacterial, Molecular detection of bacteria, PCR, Synergistic effects, Copper oxide, Titanium oxide, FESEM, EDS, XRD

Introduction

All currently available and developing medical and biological technologies are very susceptible to microbial contamination and illness. While bacterial colonization and biofilms on surfaces are directly connected to nosocomial and device-associated infections, they are often the main causes of death. Therefore, the importance of using nanoparticles as alternatives to other traditional methods such as antibiotics has emerged [1,2]. According to Mahapatra *et al.* [3], the majority of the bacterial species isolated from pipelines, including *Pseudomonas spp*., Acinetobacter spp., and Klebsiella spp., were strong biofilm builders. Moreover, the virulence and resistance of the bacteria in biofilms increased, possibly lowering the LD 50 by boosting the amount of viable bacterial cells [4]. Synergistic antibacterial mechanisms and coating application of some dioxide nanoparticles were also reported [5,6]. Similarly, Copper and Titanium nanocomposites have attracted interest due to their possible applications in cosmetics, catalysis, optoelectronic devices, sensing, magnetism fields, biomedical fields, antibacterial materials, stability, nontoxicity, and easy availability [7,8]. In recent years, TiO_2 nanoparticles have been widely used in industrial and consumer products due to their effective catalytic activity. This increase in catalytic activity has been attributed to their smaller sizes, which has allowed for a larger surface area per unit mass [9]. A significant advantage of TiO_2 is the creation of a heterojunction on reaction with another material [10]. In these kinds of applications, a significant variable is the specific surface area, which is strongly related to the NP morphology [11,12]. TiO_2 is an n-type semiconductor with an in-width band gap ranging from 3.2 to 3.6 eV [13-15]. Copper oxide finds broad applications in a wide range of different technologies, such as catalysis, energy conversion, magnetic storage, energy storage, termites, as well as superconductors [16]. CuO is a narrow band-gap (1.2 eV) p-type semiconductor with photoconductive and photochemical characteristics and has observed applications in gas sensing,

catalysis, and as an antibacterial. Agent [17,18]. In 2013, Nguyen *et al.* were prepared and characterization of nano CuO and CuO-TiO_2 photocatalysts. Their results showed that the reaction temperature and the molar ratio of the precursors play important roles in controlling the morphology and size of both CuO and CuO-TiO_2 nanocrystals [19]. In 2020, Monika *et al.* reported the synthesis of TiO_2-CuO core-shell nanoparticles for photovoltaic applications. They found good absorption efficiency and electrical properties of TiO_2-CuO [20]. In 2020, Nuha *et al*. prepared and studied TiO_2-CuO nanoparticles, They concluded that the degradation rate constants values were calculated and were 0.01391 and 0.01816 min^{-1} for CuO and TiO_2- CuO respectively [21]. In this work, the oxide nanostructures were characterized by, FESEM, EDS spectrum, and XRD.

Materials and methods

Titanium dioxide nanoparticles (US Research Nanomaterials, Inc) (Alfa Aesar, Germany) high purity 99 %, particle size 10 - 30 nm and Copper oxide nano nanoparticles (NANOSHEL), particle size less than 80 nm were used. In order to understand the transformation mechanism of the mixture CuO-TiO_2. Copper oxide was mixed with Titanium dioxide nanoparticles by different weight ratios (25, 50 and 75 % CuO-TiO_2). Then the samples were placed inside the small boxes and mixed very well within 30 min to provide fine and homogeneous particles by ion-exchanged Copper and Titanium dioxide. Both pure oxide nanoparticles and nanocomposite materials were generated in the same way through experimental stages.

Chemicals and pure material

Bacterial media and nanoparticles oxide (235533 anatases, 99.6 % trace metals basis, CAS Number 1376-70-0) were purchased from Sigma-Aldrich (Te, USA). Reagents of the *in vivo* study were bought from scientific laboratory supplies (UK). Following the manufacturer's instructions, the culture media was prepared, its (pH) was adjusted, and then it was autoclaved to sterilize it. Mueller Hinton Agar (MHA) and other media were purchased from Fluka, Switzerland.

Microorganisms

Different Gram-negative and Gram-positive, were tested, namely, *Staphylococcus aureus*, *Klebsiella pneumoniae, Pseudomonas aeruginosa*, *Bacillus subtilis*, and 4 strains of *Rhizobium sp*. All the strains were kindly identified and provided by the Microbiology Department's strain bank of the College of Education for Pure Sciences. *Rhizobium* strains were isolated from the soil and were diagnosed in the laboratory. A control sample saturated with sterile distilled water was prepared and 3 replicates were made for each treatment [22].

Identification of bacterial isolates

Bergey's Manual of Systematics of Each Bacteria was used to identify the chosen bacteria using morphological, cultural, and biochemical tests. The genetic sequence of the bacteria was then determined based on 16S ribosomal RNA (rRNA) gene sequencing using universal primers 27 F (5′-AGAGTTTGATCMTGGCTCAG-3′) and 1492 R (5′-TACGGYTACCTTGTTACGACTT-3′) as a forward primer and reverse primer respectively (Eurofins Genomics Germany) were used. DNA extraction was done using the protocol of Bacterial Xpress Nucleic Acid Extraction Kit (3096 Millipore, Chemicon®). The polymerase chain reaction (PCR) product was cleaned up using the Sigma-Aldrich PCR Purification Kit (MBD0022 Sigma-Aldrich®). Agarose gel (1 %) (05066-50G Sigma-Aldrich Gillingham) was used to electrophorese the PCR product. By using the direct PCR sequencing method, the nucleotide sequence of the bacteria's 16S rRNA gene was determined by Eurofins Sanger sequencing. The cycling circumstances of PCR were according to the following: 94 °C for 10 min and 34 cycles of denaturation at 95 °C for 30 s, annealing extension at 56 °C for 1 min, 72 °C for 1 min, and an extension at 72 °C for 10 min. BLAST analysis was used to compare the 16S rRNA gene sequence with that in the NCBI GenBank database. https://www.ncbi.nlm.nih.gov/genbank/genomesubmit/ and cluster analysis and phylogenetic tree performed by using MEGA-X program version 10.02.06 [23].

Disk diffusion assay to estimate the influence of NPs on the viability of bacteria

The disc agar diffusion (DAD) test was used to assess the *in vitro* antibacterial properties of the NPs. A separate standard paper disc was further impregnated to determine NP effects with a concentration of NP (50, 75, 100 % CuO-TiO_2). In each chosen broth medium, a single sample strain colony was cultivated overnight on a rotary shaker (180 rpm) at 28 °C. The inoculums were created by

diluting the overnight cultures and implemented to the Petri dish together with the prepared disks, that contained NP examined concentration and standard our culture collection was used as test strains. Following incubation at 37 °C for 24 h for pathogenic bacteria, and at 28 °C for 48 h for the soil bacteria, The studied bacteria were initially cultured for 1 h to serially dilution-standardize the culture to 104 CFU/mL. 25 % CuO/TiO_2 of bacteria were separated on the surface of the KBA agar plates after they had been prepared for the cultures. The sterile filter paper discs 6 mm in diameter were put on all these plates, as well as 25 µl of (0, 25, 50 and 100 % CuO-TiO_2) NPs suspended in de-ionized water were added to each filter paper disc. The inhibition zones were calculated. The tests were performed in triplicate.

Results and discussion

Surface properties

Titanium and Copper oxide nanostructures can be observed from FESEM images in **Figures 1(a) - 1(b)**. It is clear the molecular structure has completely gone leaving behind irregularly shaped particles with mean diameters of 25.35 and 34.38 nm respectively. After the mixture process, the morphology of the particle reveals seed-like structures and the atoms of titanium, oxygen and copper are uniformly distributed at the surface into the CuO-TiO_2 layer heterojunction. It indicates these elements are providing strong support for a successful ion-exchange process as the **Figures 1(c) - 1(e)**. Furthermore, the spherical aggregations of CuO nanoparticles produce some elongated particles at the surface with average sizes of 44.66, 39.11 and 37.54 nm at 25, 50 and 75 % CuO respectively. EDS analysis displays a strong signal from elements Ti, O and C also a weak signal from C and N atoms were observed in **Figure 2(a)**. In the same manner, the elements of Cu, O and C were clearly as **Figure 2(b)**. The energy position of the element Cu was found to be 8.070 keV while the element Ti was found to be 4.540 keV as **Figure 2(b)**. The chemical structure of CuO-TiO_2 nanocomposite was scanned by EDS spectrum using 25, 50 and 75 % CuO-TiO_2 as shown in **Figures 2(c) - 2(e)**. It is clear the copper nanoparticles have diffused into the surface of titanium from different regions. On the other side, the elements mapping of N, Na and Ne were presented with very small amounts. The nanocomposite increases after the mixture due to elongated particles of CuO-TiO_2 at the surface during the preparation process. The presence of copper nanoparticles can improve the process of transporting electrons at the surface and copper atoms reduce surface defects and modify it to a more homogeneously as the **Table 1** [24,25].

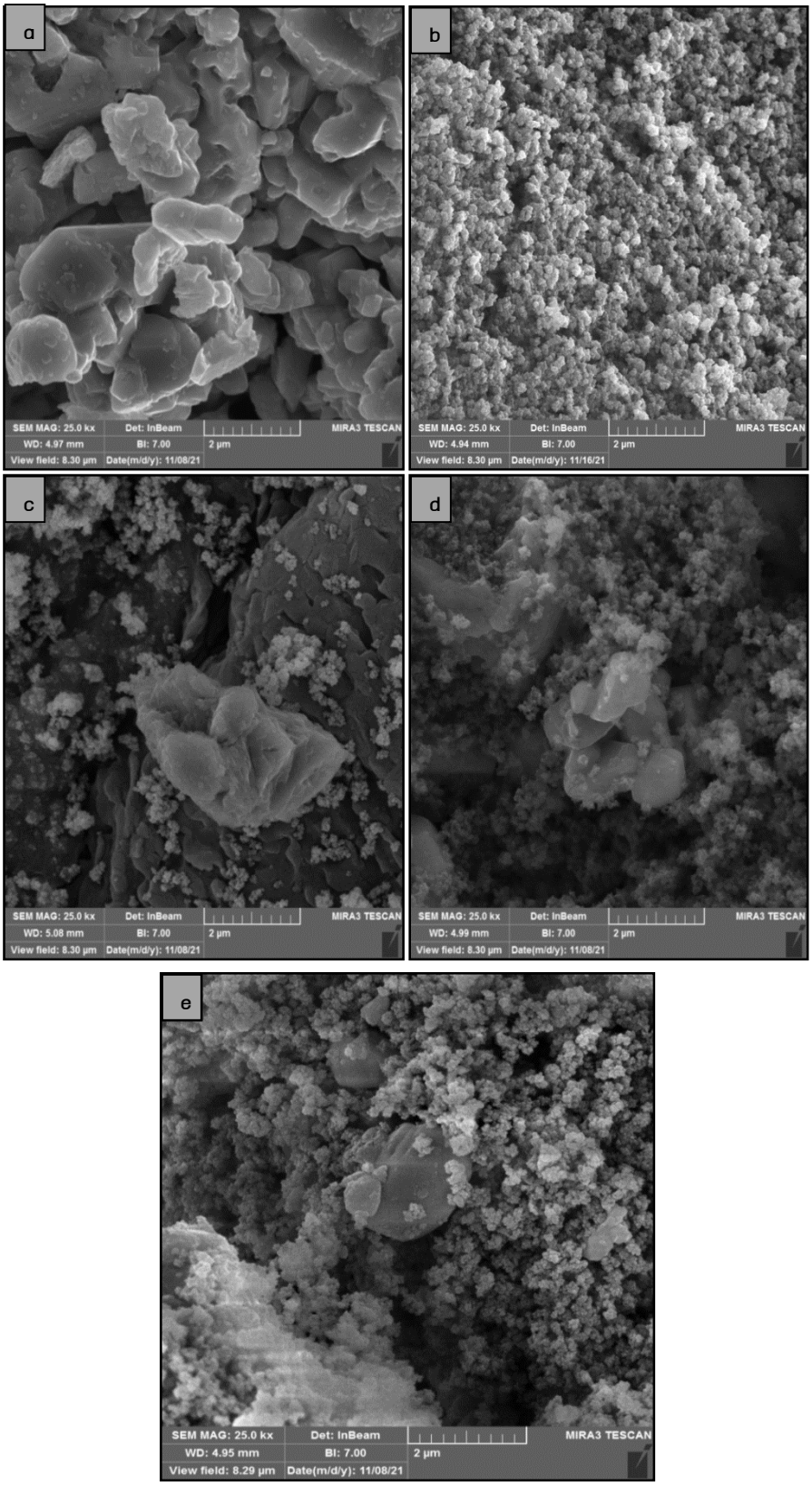

Figure 1 FESEM images (a) CuO pure, (b) TiO_2 pure, (c) 25 % CuO/TiO_2, (d) 50 % CuO/TiO_2, and (e) 75 % CuO/TiO_2.

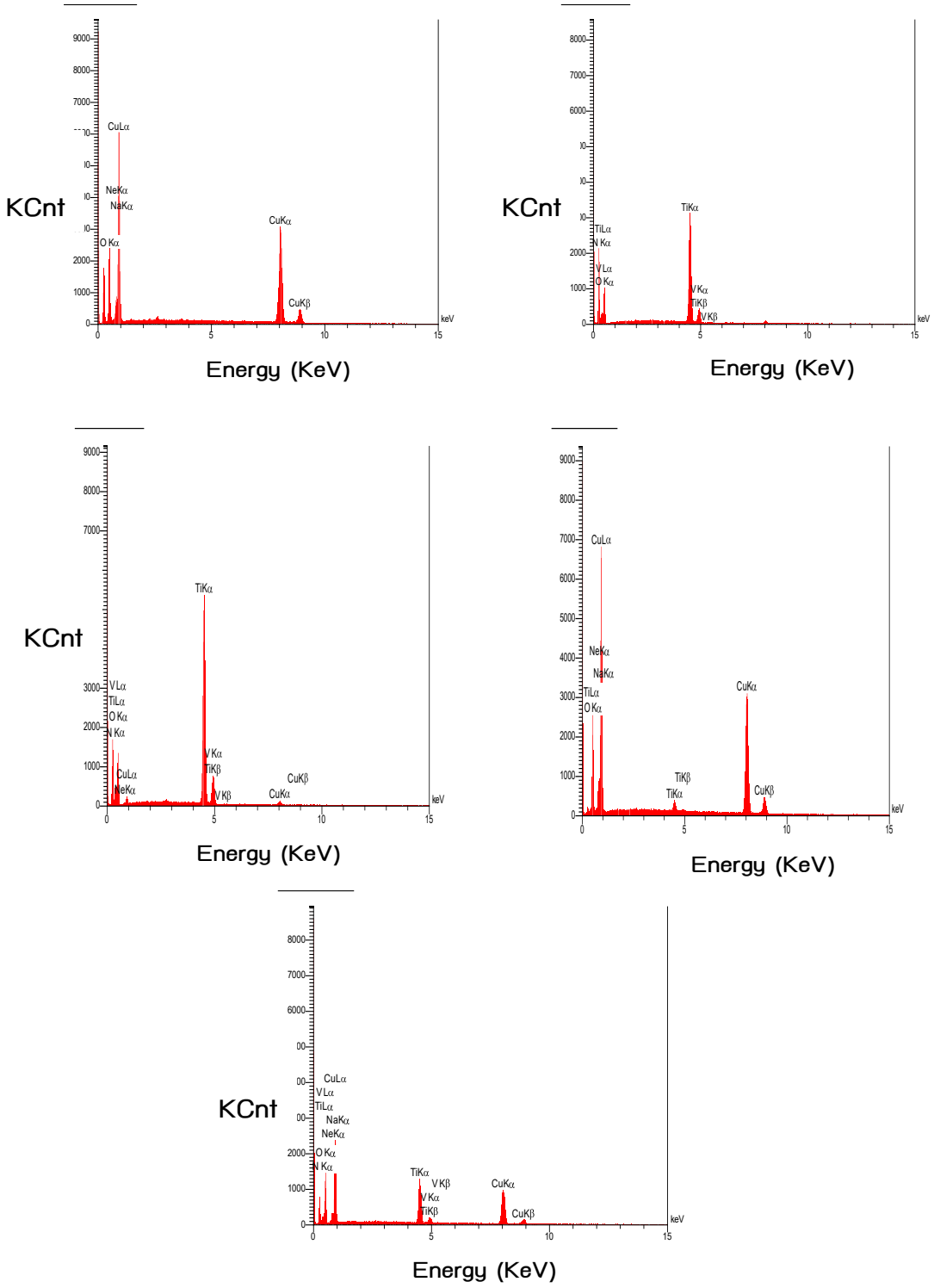

Figure 2 EDS analysis of (a) pure CuO, (b) pure TiO_2, (c) 25 % CuO-TiO_2, and (d) 25 % CuO-TiO_2, and (e) 75 % CuO-TiO_2.

Table 1 Data of elements of CuO and TiO_2, 25, 50, 75 % CuO-TiO_2 nanostructures.

Element	W % CuO	Line	W % TiO_2	W % 25 %CuO-TiO_2	W % 50 % CuO-TiO_2	W % 75 % CuO-TiO_2
C	23.61	Ka	19.71	12.58	13.71	4.43
N	-	-	4.73	4.01	3.82	-
O	28.16	Ka	39.10	36.54	39.35	29.13
Ne	4.24	Ka	-	1.14	2.58	5.62
Ti	-	-	36.46	43.41	16.18	2.64
V	-	-	0.00	1.12	0.00	-
Cu	41.62	Ka	-	1.20	21.90	54.72
	100.00		**100.00**	**100.00**	**100.00**	**100.00**

Structure properties

The Structural characteristics of CuO/TiO_2 were investigated by X-ray diffraction. The XRD pattern shows highlighted and strong peaks in the formation of TiO_2 and CuO nanostructures as **Figures 3(a) - 3(b)**. The diffraction peaks of CuO were 2θ = 27.59, 35.66, 36.25, 41.42, 48.95, 54.38, 56.76, 61.63 and 69.086 ° with orientations of (021), (002), (111), (200), (202), (020), (202), (106) and (112) respectively. Furthermore, the diffraction peaks of the TiO_2 were 2θ = 27.6, 36.28, 41.46, 54.46, 56.8 and 69.15 ° with orientations of (110), (101), (111), (105), (211) and (310) respectively. It can be seen that TiO_2 oxide has a rutile phase and copper oxide which can be indexed to (JCPDS no. 01-078-2486) [26,27]. The diffraction peaks of the CuO-TiO_2 at 2θ = 35.61, 38.78, 48.83, 61.59 and 68.13 ° can be attributed to the formation of CuO crystal phases with plane orientations of (002), (111), (202), (106) and (112) respectively. The copper oxide was successfully deposited on the TiO_2 oxide. The rutile phase was also presented in the ion-exchanged Copper Titanate as in **Figures 7(c) - 7(e)**. It is obvious that verifying the presence of rutile and copper in the composited material [28]. The incorporation ratios of copper oxide reduce surface defects and to improve the crystal phase. The average crystalline size can be evaluated according to the Scherrer equation [29].

$$L = \frac{k\lambda}{Bcos\theta} \quad (1)$$

where B is FWHM and k is a constant (k = 0.954) and L is crystallite size (nm). It is clear the crystalline size decreases after the mixture process, which could be due to the widening of the XRD peaks of copper titanates. **Tables 2** and **3** show summarize data of CuO, TiO_2 and CuO/TiO_2.

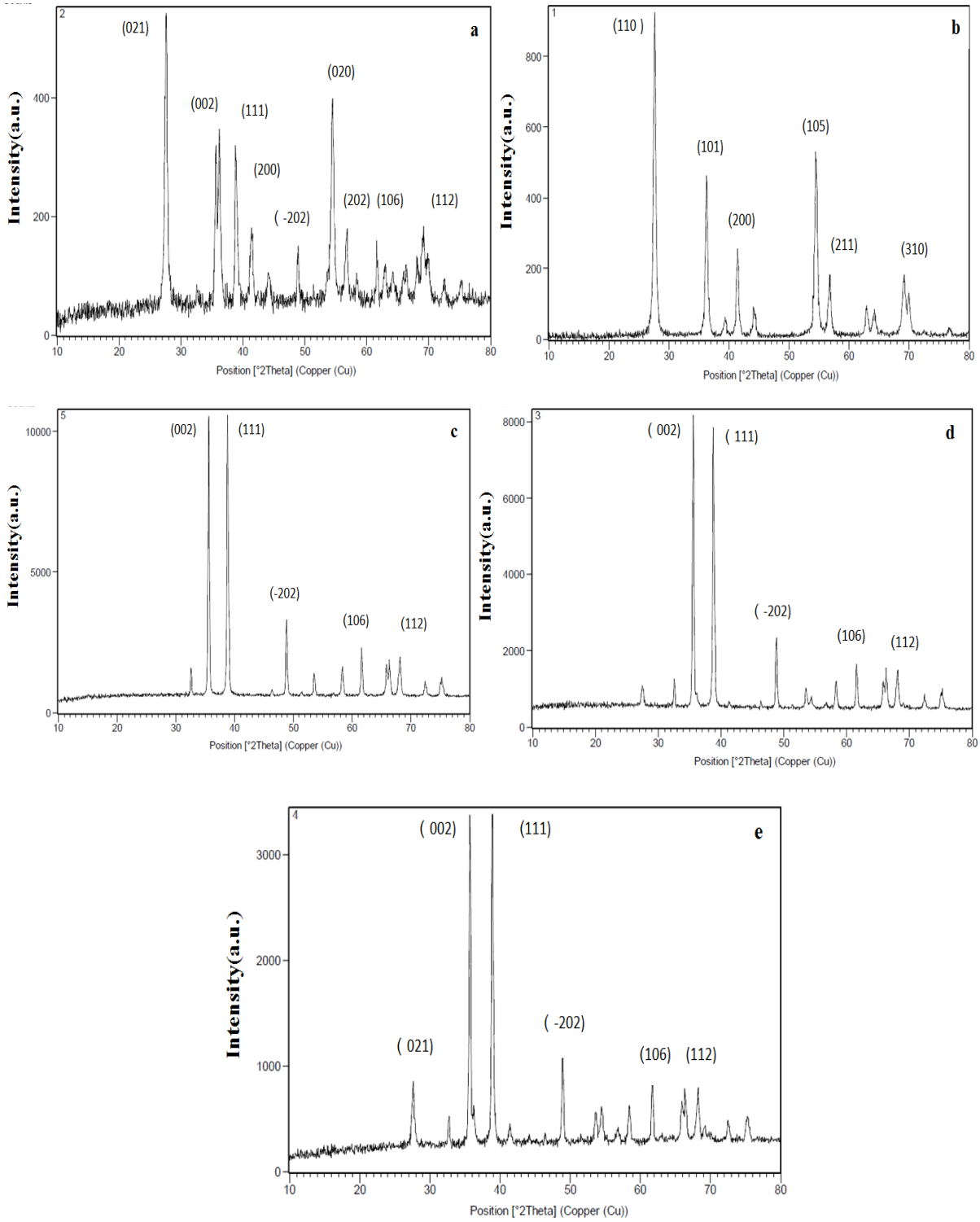

Figure 3 XRD of Copper Titanate nanostructures (a) CuO, (b) TiO_2, (c) 25 % CuO/TiO_2, (d) 50 % CuO/TiO_2, and (e) 75 % CuO/TiO_2.

Table 2 Data of elements of CuO and TiO_2 nanostructures.

2θ CuO	FWHM(deg)	L(nm)	2θ TiO_2	FWHM	L(nm)
27.5979	0.246	36.324	27.6056	0.4428	29.567
35.665	0.231	36.342	36.2894	0.2952	32.546
36.2514	0.2952	32.546	39.3988	0.3936	28.656
38.7904	0.2832	32.636	41.4694	0.3444	34.656
41.4245	0.4920	25.434	44.2396	0.4920	25.434
44.1762	0.5904	19.454	54.4690	0.4310	25.376
48.9524	0.2460	36.111	56.8088	0.4920	25.613
54.3822	0.3444	34.656	62.9260	0.4240	25.137
56.7623	0.4428	29.567	64.2250	0.3936	28.656
58.4114	0.5904	25.656	69.1551	0.3362	28.453
61.6308	0.2460	36.111	70.0026	0.3522	27.451
62.9765	0.3936	28.656			
64.2261	0.5904	19.454			
66.2124	0.4723	19.814			
69.0860	0.3936	28.656			
72.5195	0.5904	25.434			
75.2370	0.3721	24.621			

Table 3 Data of CuO-TiO_2 nanostructures.

2θ 25%CuO-TiO_2 (deg)	FWHM (deg)	L (nm)	50 %CuO CuO-TiO_2 2θ (deg)	FWHM (deg)	L (nm)	2θ 75 % CuO-TiO_2 (deg)	FWHM (deg)	L (nm)
32.5853	0.1476	48.563	27.5507	0.3936	28.656	27.6547	0.3444	34.656
35.6171	0.246	36.324	32.5720	0.1968	39.452	32.7065	0.1968	39.452
38.7817	0.246	36.324	35.5861	0.2460	36.324	35.7225	0.2460	36.324
46.3390	0.246	36.324	38.7642	0.1968	39.452	36.3176	0.1476	48.563
48.8312	0.246	36.324	41.3021	0.2952	32.546	38.8901	0.2460	36.324
51.4155	0.3936	28.656	46.3240	0.2460	36.324	41.40 48	0.3936	28.656
53.5336	0.2460	36.324	53.5064	0.2460	36.324	46.4600	0.2952	32.546
58.3295	0.2952	32.546	54.3767	0.2952	32.546	48.9327	0.2460	36.324
61.5930	0.2952	32.546	56.7145	0.3936	28.656	53.6680	0.2952	32.546
65.8324	0.1968	39.452	58.3133	0.2952	32.546	54.4629	0.2952	32.546
66.3045	0.2952	32.546	61.5887	0.2952	32.546	58.4528	0.2952	32.546
68.1375	0.2952	32.546	65.8110	0.2460	36.324	61.6842	0.2952	32.546
72.4304	0.1968	39.452	66.2859	0.1968	39.452	65.9294	0.1968	39.452
75.0019	0.1800	41.543	68.0980	0.1968	39.452	66.3986	0.1968	39.452
75.2978	0.1476	48.563	72.4140	0.1968	39.452	68.2337	0.2952	32.546
-	-	-	75.2370	0.4920	25.434	72.5635	0.2952	32.546

Influence of NPs on the viability of bacteria

A clear pattern emerged from the data of **Tables 4** and **5**, it can be noticed that the treatment of pathogenic and rhizobium bacteria with nanoparticles indicated no response at lower concentrations of 25 µg/mL. This is visibly illustrated in **Table 8**. However, when treating both pathogenic and non-pathogenic bacteria with a combination of copper nanoparticles and titanium nanoparticles, an insignificant impact on bacterial growth was noticed at the concentration of 25 µg/mL. On the contrary, **Table 6** indicates a stimulating effect on growth and no major effect on rhizobium bacteria. According to **Table 6**, it can be inferred that the best concentration was obtained when using a combination of copper nanoparticles, and titanium nanoparticles, with a colonization area of 23 cm. As for **Table 7**, it can be noticed that the influence was also obvious when using a mixture of nanoparticles at a concentration of 100 mg, although not as declared as the effect observed in **Table 10**. From **Table 7**, it is clear that the combination of nanoparticles has a significant impact on increasing the inhibition zone with *Pseudomonas aeruginosa* bacteria. The inhibition zone reached 21.9 mm at a concentration of 50 % CuO-TiO_2 and 22.3 % at a concentration of 75 % CuO-TiO_2. These inhibition zones are considered large compared to other isolates of the bacteria. Similarly, *Rhizobium sp*.2 bacteria exhibited a significant inhibition zone of 20.5 and 22.6 mm at 50 % and 75 % of CuO-TiO_2, respectively. Our findings are consistent with the earlier study of Ashok, Hao and Li [8,9,11]. Certainly, the use of NPs in inhibiting bacterial growth has been a main topic in recent years. Both copper and titanium NPs have shown promising results in this field. From the available information, it appears that both copper and titanium NPs have inhibitory effects on bacterial growth. On the other hand, copper NPs are effective in reducing and inhibiting bacterial growth. These results are consistent with other studies [26,30]. Copper nanoparticles can inhibit bacterial growth due to their ability to disrupt bacterial cell membranes and disrupt vital functions. A study published in the International Journal of Molecular Sciences showed that copper nanoparticles can inhibit the reproduction of *E. coli*, giving it a tool which can inhibit bacterial infection [31]. On the other hand, the generation of the tribes The medium inhibits bacterial growth, which produces a special free radical that damages bacterial cells Copper and titanium NPs have been studied in terms of potential they can inhibit the growth of pathogenic microorganisms. Scientists have investigated the antimicrobial behaviour of titanium nanoparticles and their ability to prevent harmful bacteria from attaching and growing [32,33], but copper nanoparticles have also shown antimicrobial activity and studied their ability to damage bacterial cell membranes and stop bacterial growth. It is important to keep in mind several factors such as the size and shape of NPs[30, 33].

Table 4 The biological activity of the Synergistic NPs against several bacteria isolates, according to the rate of inhibition zone (mm), using the concentration of 25, 50, 100 µg/mL.

Bacterial specimen	**The mean diameter of the Inhibition Zone mm ± SD for samples that were treated with CuO**			**The mean diameter of the Inhibition Zone mm ± SD for samples that were treated with TiO_2**		
	25 µg/mL CuO	**50 µg/mL CuO**	**100 µg/mL CuO**	**25 µg/mL TiO_2**	**50 µg/mL TiO_2**	**100 µg/mL TiO_2**
control group	0.00	0.00	0.00	0.00	0.00	0.00
Staphylococcus aureus	6.3 ± 1.6	16.3 ± 1.6	17.5 ± 0.67	1.3 ± 0.68	15.3 ± 0.65	16.3 ± 1.6
Klebsiella pneumoniae	9.2 ± 0.67	11.53 ± 0.67	11.3 ± 0.68	2.3 ± 1.6	16.3 ± 1.1	15.3 ± 0.57
Pseudomonas aeruginosa,	1.7 ± 0.7	15.73 ± 0.8	14.3 ± 1.37	5.3 ± 0.25	14.3 ± 0.51	17.3 ± 0.48
Bacillus subtilis	2.9 ± 1.33	16.3 ± 1.33	14.3 ± 0.30	9.3 ± 0.73	14.3 ± 0.6	16.3 ± 1.6
Rhizobium sp 1	2.63 ± 0.61	8.3 ± 0.47	15.3 ± 0.29	6.3 ± 1.6	13.3 ± 1.34	17.3 ± 0.67
Rhizobium sp 2	3.23 ± 0.68	15.36 ± 0.69	16.3 ± 1.6	9.3 ± 0.67	11.3 ± 0.67	16.22 ± 0.38
Rhizobium sp 3	2.3 ± 1.6	16.3 ± 1.1	16.3 ± 0.57	97.3 ± 0.7	14.5 ± 0.8	18.37 ± 1.34
Rhizobium sp 4	4.3 ± 0.55	16.63 ± 0.51	15.3 ± 0.48	13.3 ± 1.13	13.3 ± 1.35	17.53 ± 0.77

Table 5 The biological activity of the Synergistic nanoparticles against different bacteria isolates, according to the rate of inhibition zone (mm), using concentration 25 µg/mL.

Bacterial specimen	Mean diameter of Inhibition Zone mm ± SD		
	25% CuO	**50 % CuO**	**75 % CuO**
control group	0.00	0.00	0.00
Staphylococcus aureus	6.3 ± 1.6	16.3 ± 1.6	21.3 ± 0.67
Klebsiella pneumoniae	7.3 ± 0.28	22.8 ± 0.62	23.3 ± 0.28
Pseudomonas aeruginosa,	9.89 ± 0.7	12.3 ± 0.7	22.3 ± 1.34
Bacillus subtilis	10.3 ± 1.33	15.3 ± 1.33	19.3 ± 0.67
Rhizobium sp 1	6.9 ± 0.61	15.5 ± 0.63	21.6 ± 0.18
Rhizobium sp 2	8.3 ± 0.64	17.13 ± 0.69	19.6 ± 3.6
Rhizobium sp 3	4.3 ± 1.6	18.3 ± 1.1	22.3 ± 0.57
Rhizobium sp 4	5.3 ± 0.55	19.9 ± 0.51	21.8 ± 0.48

Table 6 The biological activity of the TiO nanoparticles against different bacteria isolates, according to the rate of inhibition zone (mm), using a concentration of 50 µg/mL.

Bacterial specimen	Zone of Inhibition (mm)		
	25 % CuO	**50 % CuO**	**75 % CuO**
control group	0.00	0.00	0.00
Staphylococcus aureus	11.3 ± 0.67	22.3 ± 0.7	21.3 ± 0.66
Klebsiella pneumoniae	13.3 ± 0.7	18.3 ± 1.37	19.3 ± 1.39
Pseudomonas aeruginosa,	14.3 ± 1.39	21.3 ± 0.92	21.1 ± 0.69
Bacillus subtilis	11.3 ± 0.67	19.3 ± 0.66	15.3 ± 1.60
Rhizobium sp 1	09.7 ± 0.69	18.2 ± 1.6	22.3 ± 1.22
Rhizobium sp 2	04.3 ± 1.23	19.3 ± 0.57	19.3 ± 0.54
Rhizobium sp 3	09.5 ± 0.57	17.3 ± 1.22	12.3 ± 2.48
Rhizobium sp 4	13.3 ± 1.24	19.6 ± 1.88	19.3 ± 0.89

Table 7 The biological activity of the Synergistic nanoparticles against different bacteria isolates, according to the rate of inhibition zone (mm), using a concentration of 100 µg/mL.

Bacterial Specimen	Zone of Inhibition (mm)		
	25 % CuO	**50 % CuO**	**75 % CuO**
control group	0.00	0.00	0.00
Staphylococcus aureus	17.3 ± 0.97	18.3 ± 0.98	15.3 ± 1.18
Klebsiella pneumoniae	14.3 ± 1.2	14.5 ± 1.6	19.3 ± 0.89
Pseudomonas aeruginosa,	16.3 ± 1.33	21.9 ± 0.67	22.3 ± 0.67
Bacillus subtilis	21.3 ± 0.67	15.3 ± 0.68	15.3 ± 0.68
Rhizobium sp 1	15.3 ± 0.68	17.3 ± 1.5	18.4 ± 1.6
Rhizobium sp 2	16.3 ± 1.6	20.5 ± 0.56	22.6 ± 0.59
Rhizobium sp 3	19.3 ± 0.57	14.8 ± 0.48	14.3 ± 0.48
Rhizobium sp 4	16.3 ± 1.6	19.3 ± 0.57	21.4 ± 0.57

Confirmation of identification of bacteria by using 16S rRNA

The identification of the bacteria was verified using 16S rRNA gene sequencing. Sequences of Rhizobium sp. strain OGM3377 16S ribosomal RNA gene 98.38 % with Rhizobiaceae bacterium strain ON381306.1 with the 16S ribosomal RNA gene and were submitted to GenBank at the NCBI website as accession number (OP942239.1) it is recorded new bacterial isolation under the names of the researchers who participated in this study, https://www.ncbi.nlm.nih.gov/nuccore/OP942239. The phylogenetic analysis and BLAST program analysis using the MEGA-X muscle algorithm program version 10.02.06 [34] was used to assess the DNA resemblance of the obtained 16S rRNA gene sequence as shown in **Figure 4**.

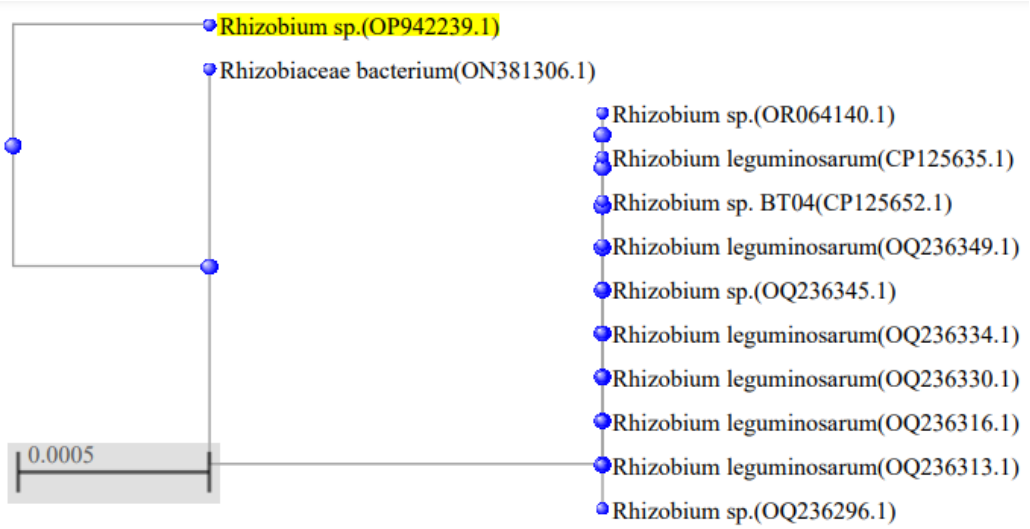

Figure 4 An algorithm that generates a tree from a set of distances (or differences) between sequences. Available options: 1) Fast minimum evolution.

Conclusions

Nanostructures CuO-TiO_2 were produced via various weight ratios. The performance of the formed nanocrystals was investigated using FESEM, EDS spectrum, and X-ray diffraction. The ratio of the molecular exchange plays an important role in controlling the size diameter and shape of CuO, TiO_2 and CuO-TiO_2 nanostructures. Additionally, the increasing reaction process leads to be highly effective in enhancing the performance nanostructures of the mixture which is expected to be harmonized by changing various parameters. The sharp peaks of the composites indicate that CuO has a high degree of crystallinity. Sequencing of the 16S rRNA gene was performed to confirm the bacteria's identity. The 16S ribosomal RNA gene sequences of Rhizobium sp. strain OGM3377 and Rhizobiaceae bacterium strain ON381306.1 were submitted to GenBank at the NCBI website and given the accession number (OP942239.1). The new bacterial isolation is listed under the names of the researchers who took part in this study. The biological efficiency of the utilised nanoparticles is enhanced by the employment of 2 different types of nanoparticles, which may have a significant effect on preventing aggregation and agglomeration in these particles. Depending on the type of nanoparticles used, the efficiency of using them against pathogenic and non-pathogenic bacteria may fluctuate. In general, bacteria are killed, and bacterial development is inhibited by the use of nanoparticles known for their antibacterial activity, such as silver and copper. Generally, the performance of different nanoparticles in combating bacteria and their influence on human health and the environment should be assessed before making any decisions regarding their use. Additionally, conducting research and necessary tests are crucial to ensure the safety and efficacy of nanoparticles in fighting bacteria. In conclusion, both copper and titanium nanoparticles have their strengths when it comes to inhibiting bacterial growth. The choice between the two would depend on various factors, including the specific needs of the application and the environment in which they will be used.

References

[1] JP Guggenbichler, O Assadian, M Boeswald and A Kramer. Incidence and clinical implication of nosocomial infections associated with implantable biomaterials-catheters, ventilator-associated pneumonia, urinary tract infections. *GMS Krankenhaushygiene Interdisziplinär* 2011; **6**, 234.

[2] L Zamora-Mendoza, E Guamba, K Miño, MP Romero, A Levoyer, JF Alvarez-Barreto and F Alexis. Antimicrobial properties of plant fibers. *Molecules* 2022; **27**, 7999.

[3] A Mahapatra, N Padhi, D Mahapatra, M Bhatt, D Sahoo, S Jena, D Dash and N Chayani. Study of biofilm in bacteria from water pipelines. *J. Clin. Diagn. Res.* 2015; **12**, 3456.

[4] D Căpățînă, B Feier, O Hosu, M Tertiș and C Cristea. Analytical methods for the characterization and diagnosis of infection with *Pseudomonas aeruginosa*: A critical review. *Anal. Chim. Acta* 2022; **12**, 339696.

[5] IE Mba and EI Nweze. Nanoparticles as therapeutic options for treating multidrug-resistant bacteria: Research progress, challenges, and prospects. *World J. Microbiol. Biotechnol.* 2021; **37**, 30.

[6] S Chen, Y Guo, H Zhong, S Chen, J Li, Z Ge and J Tang. Synergistic antibacterial mechanism and coating application of copper/titanium dioxide nanoparticles. *Chem. Eng. J.* 2014; **256**, 238-46.

[7] LC Zongjie. Improved photocatalytic activity of nanoCuO-incorporatedTiO_2 granules prepared by spray drying. *Progr. Nat. Sci. Mater. Int.* 2015; **25**, 334-41.

[8] CH Ashok, VK Rao and CC Shilpa. CuO/TiO_2 metal oxide nanocomposite synthesis *via* room temperature ionic liquid. *J. Nanomaterials Mol. Nanotechnology* 2016; **5**, 2-4.

[9] H Shi, R Magaye, V Castranova and J Zhao. Titanium dioxide nanoparticles: A review of current toxicological data. *Part. Fibre Toxicol.* 2013; **10**, 1-33.

[10] R Laith, GG Ali and MH Younusand. Evaluation of optical and electrical properties of TiO_2 thin films doped Cu ions. *AIP Conf. Proc.* 2019; **2201**, 020001.

[11] DLi, C Hongwei, W Xiao, L Ying, Z Shengzhi and L Dechun. Enhanced broadband nonlinear optical response of TiO_2/CuO nanosheets via oxygen vacancy engineering. *Nanophotonics* 2021; **10**, 232.

[12] T Hao. 2014, TiO_2-supported copper nanoparticles prepared via ion exchange for photocatalytic hydrogen production. Ph. D. Dissertation. The University of New South Wales, Kensington, Australia.

[13] TA Aswad, TA Abbas and GG Ali. Effect of deposition time on optical properties of CuO thin film prepared by chemical bath deposition method. *Digest J. Nanomaterials Biostructures* 2021; **16**, 831-8.

[14] Q Shi, G Ping, X Wang, H Xu, J Li, J Cui, H Abroshan, H Ding and G Li. CuO/TiO_2 heterojunction composites: An efficient photocatalyst for selective oxidation of methanol to methyl formate. *J. Mater. Chem. A* 2019; **7**, 2253-60.

[15] M Rasheed, O Alabdali and S Shihab. A new technique for solar cell parameters estimation of the single-diode model. *J. Phys. Conf.* 2021; **1879**, 032120.

[16] S Gharbi, R Dhahri, M Rasheed, E Dhahri, R Barille, M Rguiti, A Tozri and MR Berber. Effect of Bi substitution on nanostructural, morphologic, and electrical behaviour of nanocrystalline $La_{1-x}Bi_xNi_{0.5}Ti_{0.5}O_3$ (x = 0 and x = 0.2) for the electrical devices. *Mater. Sci. Eng. B* 2021; **270**, 115191.

[17] D Bouras and M Rasheed. Comparison between CrZO and AlZO thin layers and the effect of doping on the lattice properties of zinc oxide. *Opt. Quant. Electron.* 2022; **54**, 824.

[18] D Bouras, M Rasheed, R Barille and MN Aldaraj. Efficiency of adding fibers during the process of filtering solution of toxic organic dyes. *Opt. Mater*. 2022; **131**, 112725.

[19] HN Thi, LN Thu, D Thi and LN Quang. Synthesis and characterization of nano-CuO and CuO/TiO_2 photocatalysts. *Adv. Nat. Sci. Nanoscience Nanotechnology* 2013; **4**, 025002.

[20] M Monika, N Devi, S Sharma, S Tripathi and M Rani. Synthesis and study of TiO_2/CuO core-shell nanoparticles for photovoltaic applications, materi. *Mate. Today Proc.* 2020; **28**, 805.

[21] AR Nuha, KE Hanaa and MK Noor. Synthesis and characterization of CuO nanoparticles and TiO_2/CuO nanocomposite and using them as photocatalysts. *AIP Conf. Proc.* 2020; **2290**, 030006.

[22] RM El-Mekkawy, TN Almanaa, MA Yassin, G Rabie and N Saleh. Silver nanoparticles (AgNPs) biosynthesized by Aspergillus flavus KF946095; their characterization and antibacterial activity. *J. Pure Appl. Microbiol.* 2021; **15**, 105-13.

[23] S Kumar, G Stecher, M Li, C Knyaz and K Tamura. MEGA X: Molecular evolutionary genetics analysis across computing platforms. *Mol. Biol. Evol.* 2018; **35**, 1547.

[24] PE Ekane, JN Lambi and VN Beckley. Synthesis and characterization of CuO, TiO_2 and CuO-TiO_2 mixed oxide by a modified oxalate route. *J. Appl. Chem.* 2017; **3**, 4518654.

[25] Y Zeng, T Wang, S Zhang, Y Wang and Q Zhong. Sol−gel synthesis of CuO-TiO_2 catalyst with high dispersion CuO species for selective catalytic oxidation. *Appl. Surf. Sci.* 2017; **411**, 227-34.
[26] L Dongfang, AZ Osman, KA Angaw, H Qitang, C Xiaoyun and Z Yushan. Synthesis and photocatalytic activities of a CuO/TiO_2 composite catalyst using aquatic plants with accumulated copper as a template. *Royal Soc. Chem.* 2019; **9**, 356.
[27] Q Shi, Y Li, ES Zhan, N Ta and WJ Shen. Directed synthesis of anatase TiO_2 truncated bipyramids with preferential exposure of the reactive {001} facet. *CrystEngComm* 2015; **17**, 3376-82.
[28] C Yu, G Li, S Kumar, H Kawasaki and R Jin. Stable Au25(SR)18/TiO_2 composite nanostructure with enhanced visible light photocatalytic activity. *J. Phys. Chem. Lett.* 2013; **4**, 2847-52.
[29] J Edwards, B Solsona, P Landon, A Carley, A Herzing, C Kiely and G Hutchings. Direct synthesis of hydrogen peroxide from H2 and O_2 using TiO_2-supported Au−Pd catalysts. *J. Catal.* 2005; **236**, 69-79.
[30] M Azizi-Lalabadi, A Ehsani, B Divband and M Alizadeh-Sani. Antimicrobial activity of Titanium dioxide and Zinc oxide nanoparticles supported in 4A zeolite and evaluation the morphological characteristic. *Sci. Rep.* 2019; **9**, 17439.
[31] X Ma, S Zhou, X Xu and Q Du. Copper-containing nanoparticles: Mechanism of antimicrobial effect and application in dentistry-a narrative review. *Front. Surg.* 2022; **9**, 905892.
[32] R Liu, K Memarzadeh, B Chang, Y Zhang, Z Ma, RP Allaker and K Yang. Antibacterial effect of copper-bearing titanium alloy (Ti-Cu) against Streptococcus mutans and Porphyromonas gingivalis. *Sci. Rep.* 2016; **6**, 29985.
[33] UF Gunputh, H Le, K Lawton, A Besinis, C Tredwin and RD Handy. Antibacterial properties of silver nanoparticles grown in situ and anchored to titanium dioxide nanotubes on titanium implant against Staphylococcus aureus. *Nanotoxicology* 2020; **14**, 97-110.
[34] CLD Dicastillo, MG Correa, FB Martínez, C Streitt and MJ Galotto. *Antimicrobial effect of titanium dioxide nanoparticles*. *In*: M Mareș, SHE Lim, L Kok-Song and C Romeo-Teodor. Antimicrobial Resistance. IntechOpen, London, 2020.